

ZH production in gluon fusion at NLO QCD

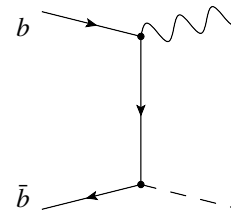
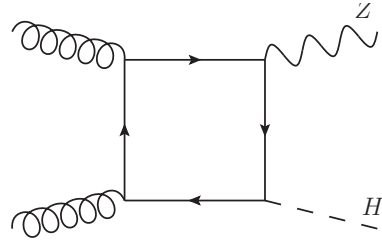
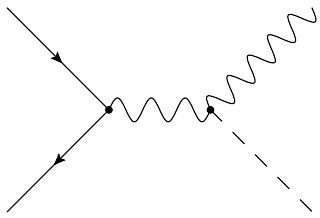
Matthias Kerner
Higgs 2022 – Pisa, 10 Nov 2022

in collaboration with
L. Chen, J. Davies, G. Heinrich, S. Jones, G. Mishima, J. Schlenk, M. Steinhauser

JHEP 08 (2022) 056 (arXiv:2204.05225)

Introduction – ZH Production Modes

ZH production modes



NNLO: Brein, Djouadi, Harlander 03

N³LO: Baglio, Duhr, Mistlberger, Szafron 22

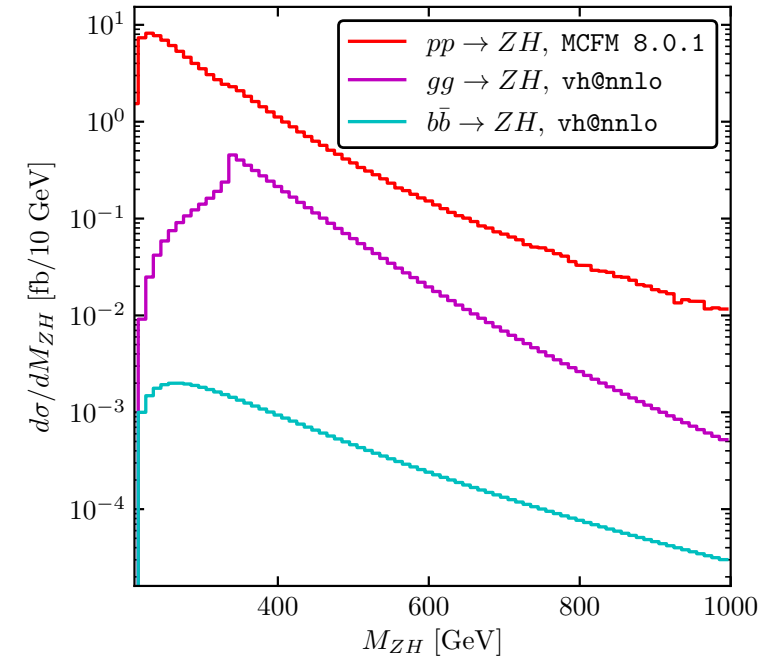
NNLO

Ahmed, Ajjath, Chen, Dhani, Mukherjee, Ravindran 19

Gluon-induced production:

- Contribution to total cross section ~10%
- Large scale uncertainties

[Harlander, Klappert, Liebler, Simon 18]



quark-initiated production
known with high accuracy:

NNLO: Brein, Harlander, Wiesemann, Zirke; Ferrera, Grazzini, Somogyi, Tramontano; Campbell, Ellis, Williams; Gauld, Gehrmann-De Rideer, Glover, Huss, Majer

NLO EW(+QCD): Ciccolini, Denner, Dittmaier, Kallweit, Krämer, Mück; Granata, Lindert, Oleari, Pozzorini; Obul, Dulat, Hou, Tursun, Yulkun

N³LO: Baglio, Duhr, Mistlberger, Szafron 22

Uncertainties in ZH, WH measurements

ATLAS 2007.02873

Signal	
Cross-section (scale)	0.7% (<i>qq</i>), 25% (<i>gg</i>)
$H \rightarrow b\bar{b}$ branching fraction	1.7%
Scale variations in STXS bins	3.0%–3.9% (<i>qq</i> → <i>WH</i>), 6.7%–12% (<i>qq</i> → <i>ZH</i>), 37%–100% (<i>gg</i> → <i>ZH</i>)
PS/UE variations in STXS bins	1%–5% for <i>qq</i> → <i>VH</i> , 5%–20% for <i>gg</i> → <i>ZH</i>
PDF+ α_S variations in STXS bins	1.8%–2.2% (<i>qq</i> → <i>WH</i>), 1.4%–1.7% (<i>qq</i> → <i>ZH</i>), 2.9%–3.3% (<i>gg</i> → <i>ZH</i>)
m_{bb} from scale variations	M+S (<i>qq</i> → <i>VH</i> , <i>gg</i> → <i>ZH</i>)
m_{bb} from PS/UE variations	M+S
m_{bb} from PDF+ α_S variations	M+S
p_T^V from NLO EW correction	M+S

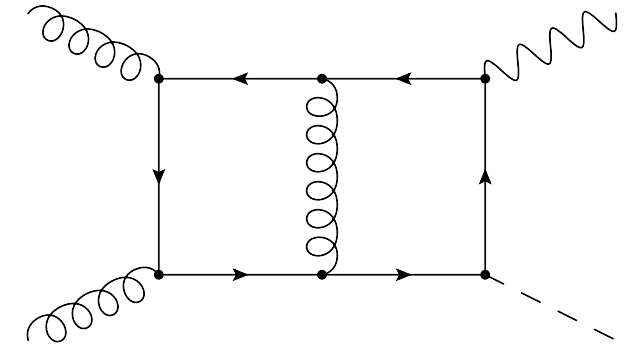
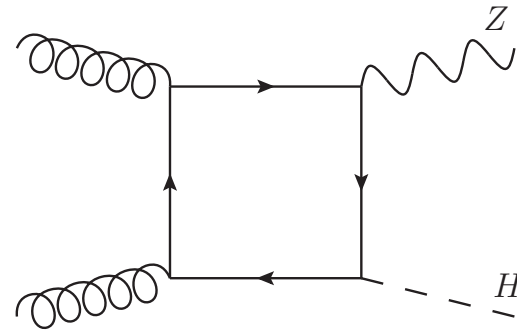
Introduction – gg → ZH: Calculations at LO and NLO

Leading Order

[Dicus, Kao 88; Kniehl 90]

NLO in $m_t \rightarrow \infty$ limit

[Altenkamp, Dittmaier, Harlander, H. Rzehak, Zirke 12]



Virtual corrections with m_t dependence

- Expansion in large m_t , up to $1/m_t^8$, improved by Padé approx.

[Hasselhuhn, Luthe, Steinhauser 17]

- expansion in small and large m_t , up to $1/m_t^{10}, m_t^{32}$ + Padé approx.

[Davies, Mishima, Steinhauser 20]

- numerical evaluation using pySecDec

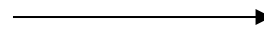
[Chen, Heinrich, Jones, MK, Klappert, Schlenk 20]

- expansion in small p_T up to p_T^4

[Alasfar, Degrassi, Giardino, Gröber, Vitti 21]

- combine expansions in small p_T and small m_t

[Bellafronte, Degrassi, Giardino, Gröber, Vitti 22]



Full NLO results:

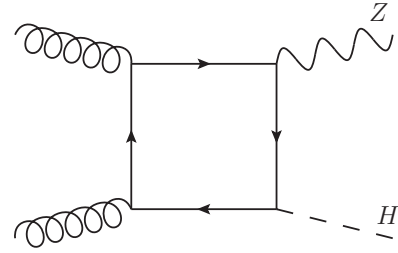
- Chen, Davies, Heinrich, Jones, MK, Mishima, Schlenk, Steinhauser 22

- Degrassi, Gröber, Vitti, Zhao 22

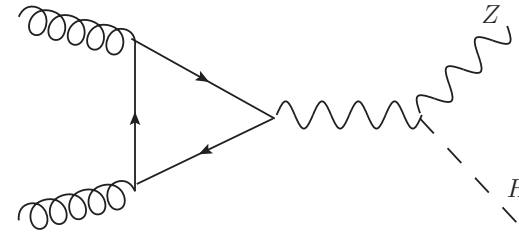
- small m_Z, m_H expansion
Wang, Xu, Xu, Yang 21

Introduction – ZH in Gluon Fusion

LO

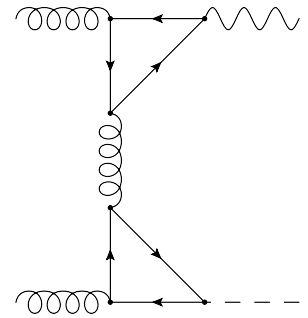
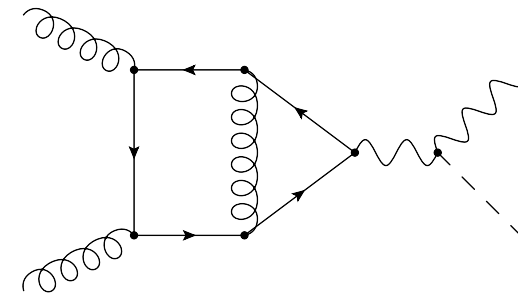
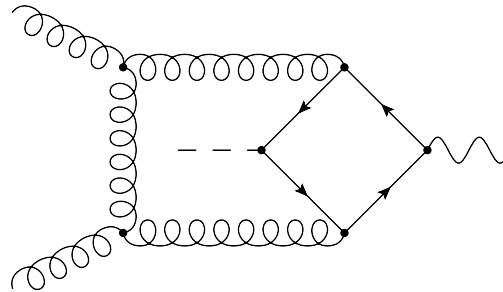
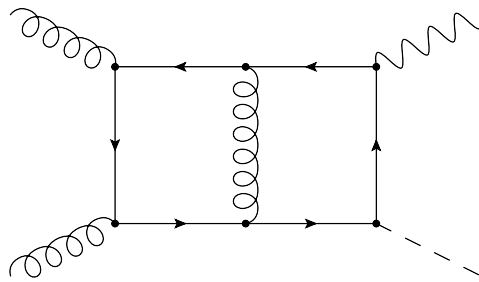


only top-quark contributing

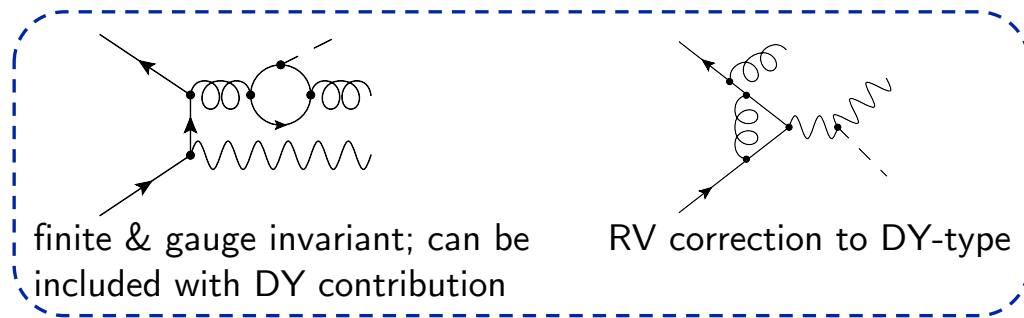
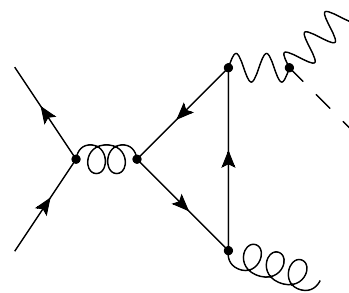
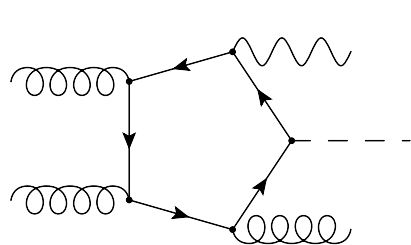


triangle contributions vanish for mass-degenerate quark doublets
 → contributions by b- and t-quark

NLO virtual



NLO reals



finite & gauge invariant; can be included with DY contribution

RV correction to DY-type

not included here

Overview of Calculation

Virtual Corrections using 2 methods:

Numerical evaluation using pySecDec
[Chen, Heinrich, Jones, MK, Klappert, Schlenk 20]

- ✓ valid for arbitrary kinematics
- ✗ evaluation challenging in HE region
- ✗ masses fixed during integral reduction
→ can only use OS mass

High-energy expansion
[Davies, Mishima, Steinhauser 20]

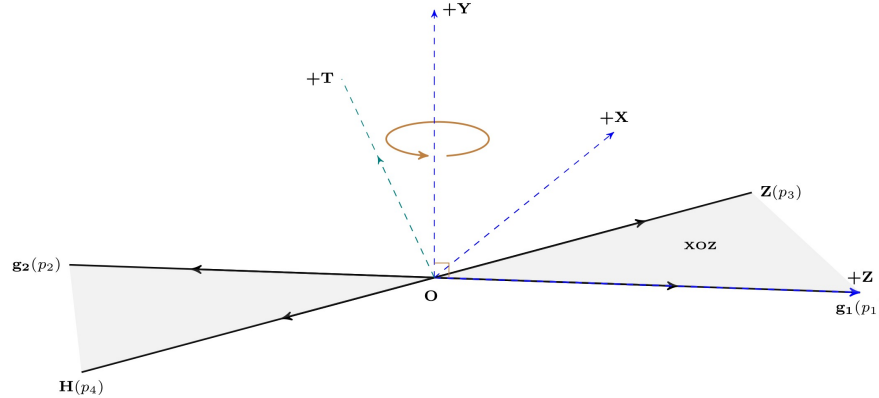
- ✗ only valid in HE region
- ✓ fast evaluation
- ✓ arbitrary masses

→ We combine these calculations at histogram level, using $p_T = 200$ GeV as a threshold

Real-radiation amplitudes generated with GoSam [Cullen et.al.]

Overview of Numerical Calculation

1) Write amplitude using linear polarizations [L. Chen 19]



$$\mathcal{A} = \varepsilon_{\lambda_1}^{\mu_1}(p_1) \varepsilon_{\lambda_2}^{\mu_2}(p_2) (\varepsilon_{\lambda_3}^{\mu_3}(p_3))^* \mathcal{A}_{\mu_1 \mu_2 \mu_3}$$

$$\varepsilon_x^\mu = \mathcal{N}_x (-s_{23} p_1^\mu - s_{13} p_2^\mu + s_{12} p_3^\mu),$$

$$\varepsilon_y^\mu = \mathcal{N}_y (\epsilon_{\mu_1 \mu_2 \mu_3}^\mu p_1^{\mu_1} p_2^{\mu_2} p_3^{\mu_3}),$$

$$\varepsilon_T^\mu = \mathcal{N}_T \left((-s_{23}(s_{13} + s_{23}) + 2m_Z^2 s_{12}) p_1^\mu + (s_{13}(s_{13} + s_{23}) - 2m_Z^2 s_{12}) p_2^\mu + s_{12}(-s_{13} + s_{23}) p_3^\mu \right),$$

$$\varepsilon_l^\mu = \mathcal{N}_l (-2m_Z^2 (p_1^\mu + p_2^\mu) + (s_{13} + s_{23}) p_3^\mu),$$

2) Use IBP-reduction to reduce all integrals to minimal set of master integrals

- using Kira [Klappert, Lange, Maierhöfer, Usovitsch] with Firefly [Klappert, Klein, Lange]

- simplification: fix $\frac{m_Z^2}{m_t^2} = \frac{23}{83}$, $\frac{m_H^2}{m_t^2} = \frac{12}{23} \rightarrow m_Z = 91.18 \text{ GeV}, m_H = 125.1 \text{ GeV}, m_t = 173.21 \text{ GeV}$

- choice of masters:

- (quasi-) finite basis [von Manteuffel, Panzer, Schabinger 14]

- simple denominators factors

- with d-dependence factorized [Smirnov, Smirnov `20; Usovitsch `20]

- ...

$$\left. \begin{array}{l} N(s, t, d) \\ D_1(d) D_2(s, t) \end{array} \right\}$$

- avoid spurious poles & cancellations

- reduced file sizes of expressions:

- amplitude: factor of 5

- most complicated coefficient:

150 MB \rightarrow 5 MB

3) Sector decompose integrals using pySecDec

4) Numerical integration using a Quasi-Monte Carlo using GPUs

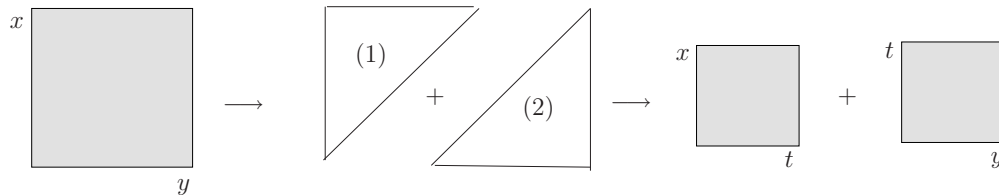
Sector Decomposition – pySecDec

Numerical evaluation of loop integrals with pySecDec

[Borowka, Heinrich, Jahn, Jones, MK, Langer, Magerya, Pöldaru, Schlenk, Villa]

Available at
github.com/gudrunhe/secdec

- Sector decomposition [Binoth, Heinrich 00] factorizes overlapping singularities



- Subtraction of poles & expansion in ϵ
- Contour deformation [Soper 00; Binoth et.al. 05, Nagy, Soper 06; Borowka et al. 12]
- Finite integrals at each order in ϵ
- Numerical integration possible

New release:

- expansion by regions
- automated reduction of contour-def. parameter
- automatically adjusts FORM settings
- evaluation of linear combinations of integrals, with automated optimization of sampling points N per sector, based on

$$T = \sum_{\text{integral } i} t_i + \lambda \left(\sigma^2 - \sum_i \sigma_i^2 \right) \quad \sigma_i = c_i \cdot t_i^{-e}$$

$\sigma_i =$ error estimate (including coefficients in amplitude)
 $\lambda =$ Lagrange multiplier $\sigma =$ precision goal

pySecDec integral libraries can be directly linked to amplitude code

Quasi-Monte Carlo Integration

Review: Dick, Kuo, Sloan 13
 First application to loop integrals:
 Li, Wang, Yan, Zhao 15

Our preferred integration algorithm is a
 Quasi-Monte Carlo using rank-1 shifted lattice rule

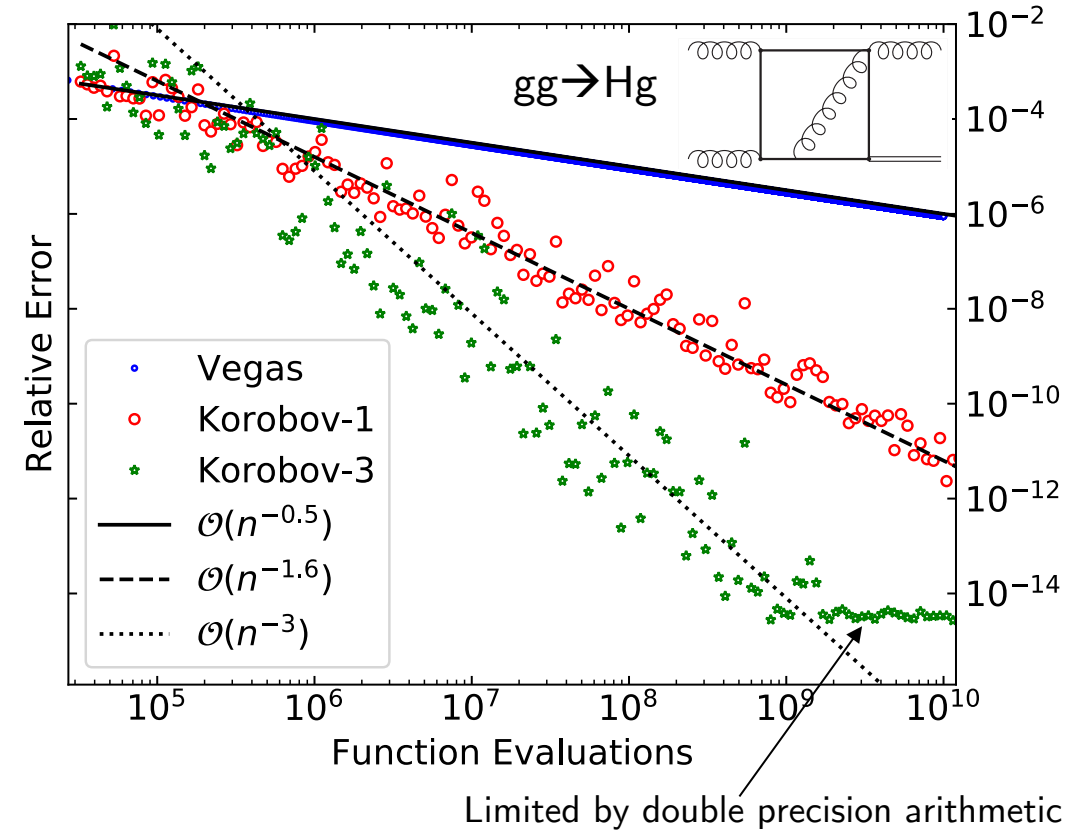
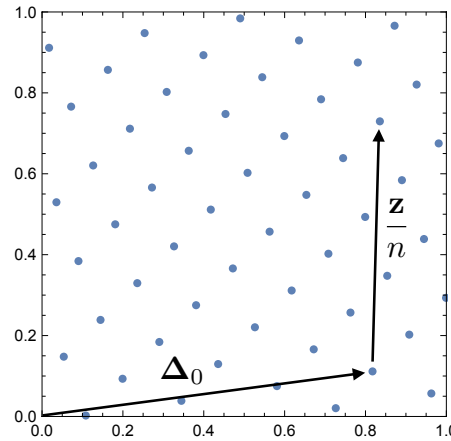
$$I[f] \approx I_k = \frac{1}{N} \cdot \sum_{i=1}^N f(\mathbf{x}_{i,k}), \quad \mathbf{x}_{i,k} = \left\{ \frac{i \cdot \mathbf{z}}{N} + \Delta_k \right\}$$

$\{\dots\}$ = fractional part ($\rightarrow x \in [0; 1]$)

Δ_k = randomized shifts
 $\rightarrow m$ different estimates of Integral
 \rightarrow error estimate of result

\mathbf{z} = generating vector
 constructed component-by-component [Nuyens 07]
 minimizing worst-case error

\rightarrow integration error scales as $\mathcal{O}(n^{-1})$ or better



High-Energy Expansion

Scale hierarchy in high-energy region:

$$m_Z, m_H < m_t \ll s, t$$

1) Use Taylor series expansion in m_Z, m_H
 → remaining integrals only depend on m_t, s, t

2) Solve differential equations using ansatz

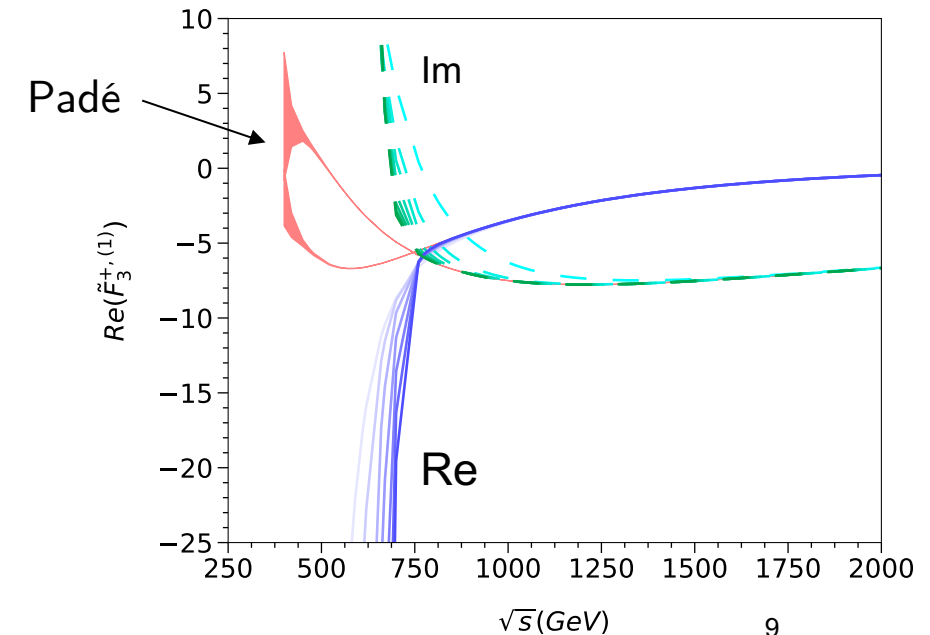
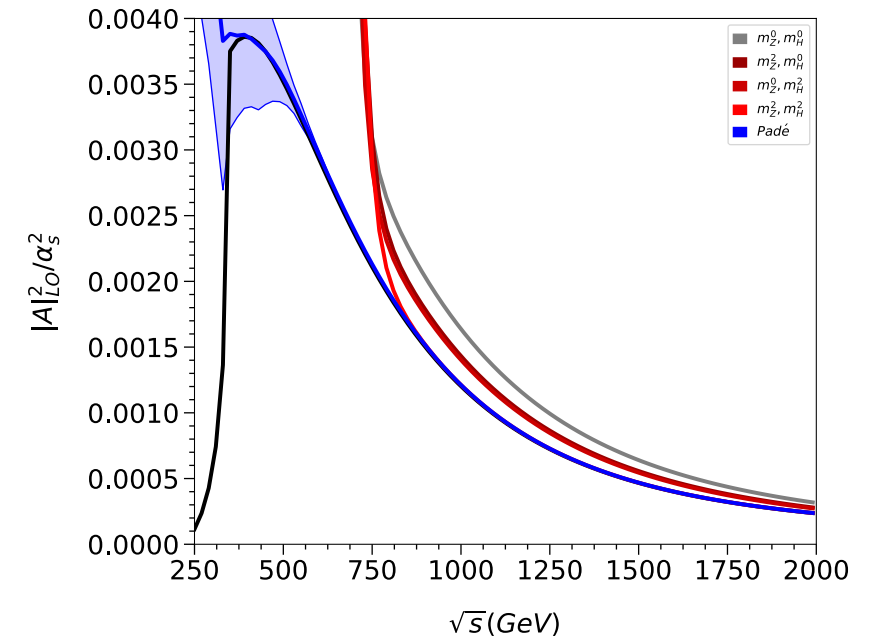
$$I = \sum_{n_1=n_1^{\min}}^{\infty} \sum_{n_2=n_2^{\min}}^{\infty} \sum_{n_3=0}^{2l+n_1} c(I, n_1, n_2, n_3, s, t) \epsilon^{n_1} (m_t^2)^{n_2} (\log(m_t^2))^{n_3}$$

3) Boundary conditions using [see Mishima 18]

- expansion-by-regions [Beneke, Smirnov; Jantzen]
- Mellin-Barnes techniques

4) Series convergence improved using Padé approximants:

$$\mathcal{V}_{\text{fin}}^N = \frac{a_0 + a_1 x + \dots + a_n x^n}{1 + b_1 x + \dots + b_m x^m} \equiv [n/m](x)$$

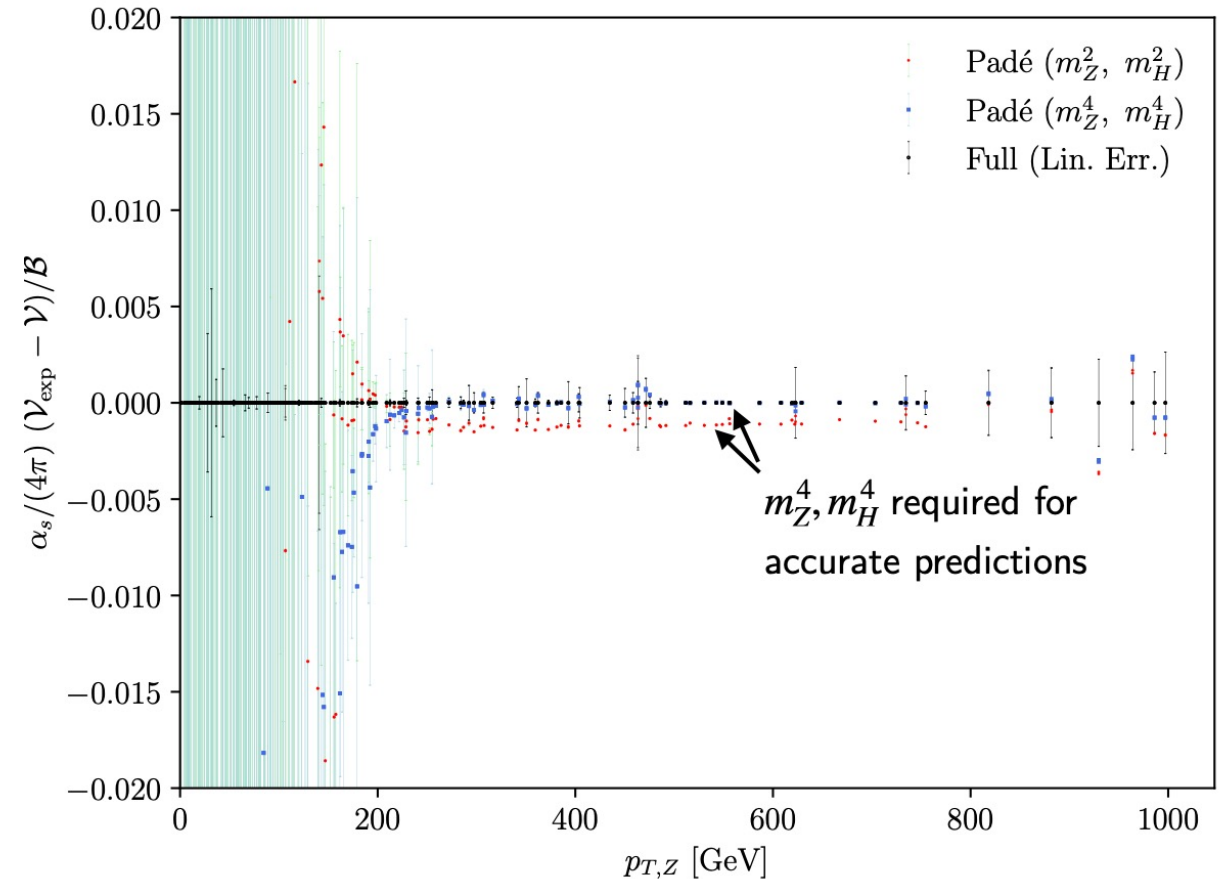


Combination with Expansions

Comparison of numerical results with high-energy expansion

- expansion around small masses up to m_t^{32}, m_Z^4, m_H^4
- agreement at 0.1% level or better for $p_T > 200$ GeV
- m_Z^4, m_H^4 terms required to reach this accuracy

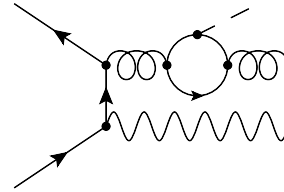
We switch from the numerical calculation
to the expansion at $p_T=200$



Results – Total Cross Section & Invariant Mass

\sqrt{s}	LO [fb]	NLO [fb]
13 TeV	$52.42^{+25.5\%}_{-19.3\%}$	$103.8(3)^{+16.4\%}_{-13.9\%}$
13.6 TeV	$58.06^{+25.1\%}_{-19.0\%}$	$114.7(3)^{+16.2\%}_{-13.7\%}$
14 TeV	$61.96^{+24.9\%}_{-18.9\%}$	$122.2(3)^{+16.1\%}_{-13.6\%}$

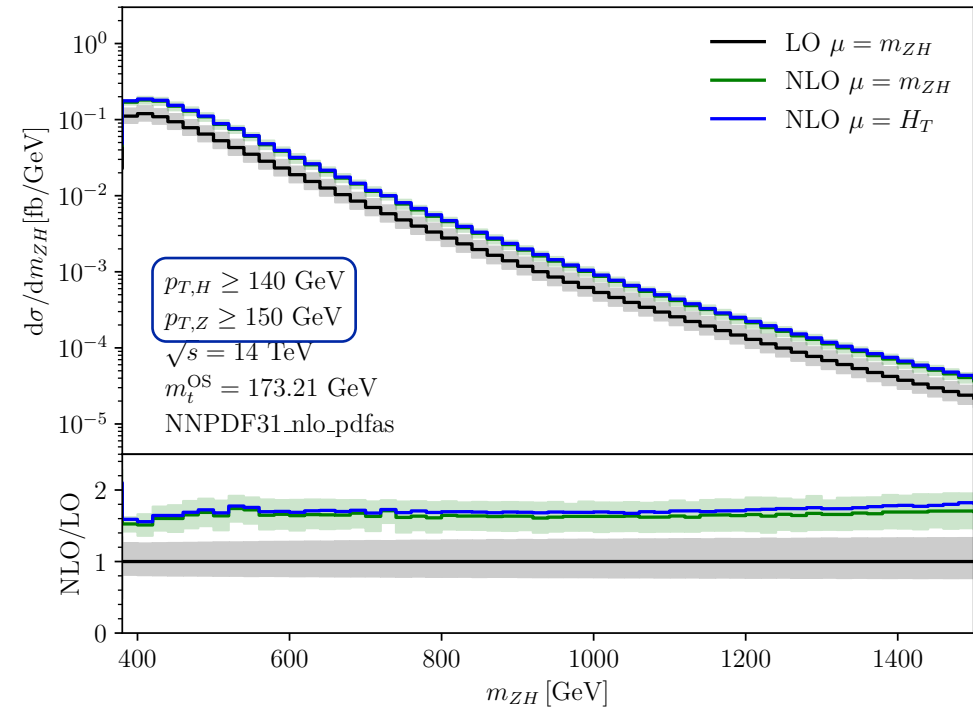
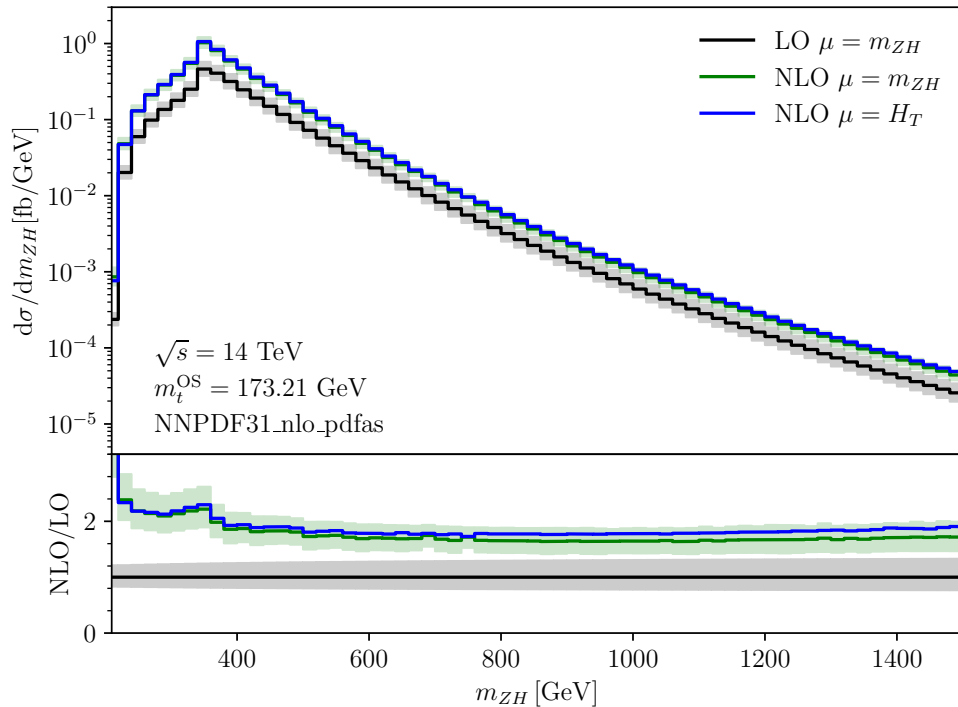
- NLO/LO ≈ 2
- NLO scale uncertainty: $\pm 15\%$
- K-factor relatively flat for $m_{ZH} > 400\text{GeV}$
larger effects at top-pair threshold and below



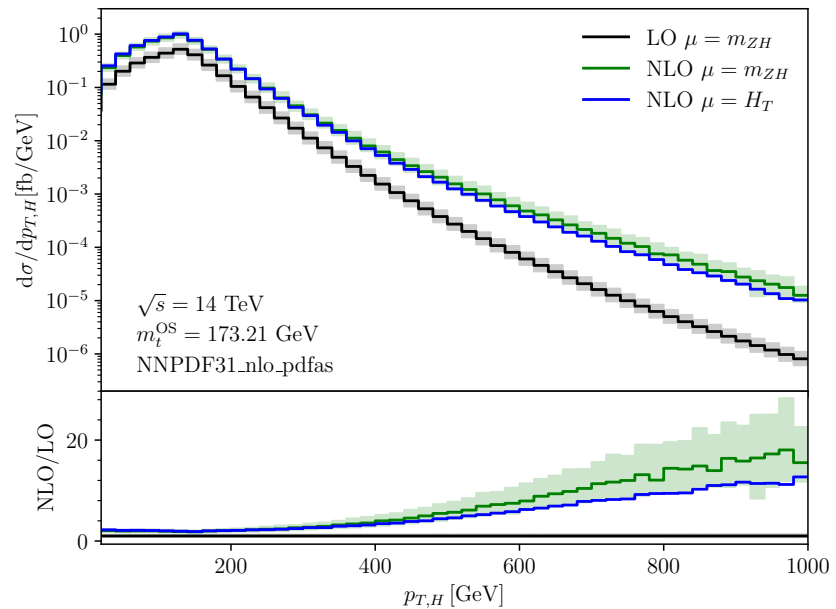
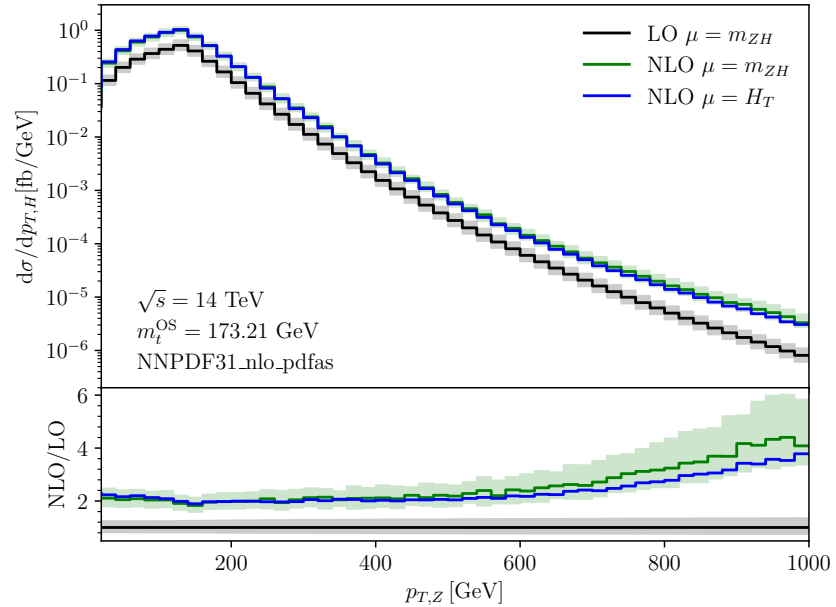
can be attributed to
 $gg \rightarrow ZH$ or DY
 → next talk

has been studied as
 part of NNLO $q\bar{q} \rightarrow ZH$ production
 see e.g. Brein, Harlander, Wiesemann, Zirke 12

included in independent
 calculation of $gg \rightarrow ZH$ production
 (formally N3LO of DY type)
 Degraasi, Gröber, Vitti, Zhao 22



Results – p_T distributions

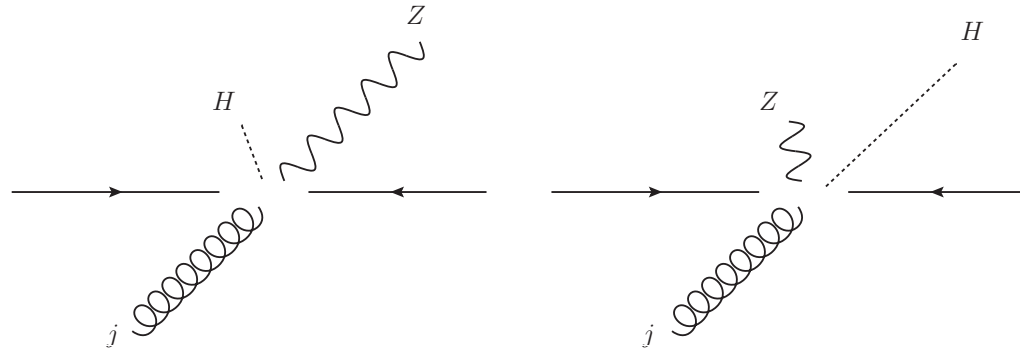


large corrections at high p_T

already observed in ZHj@LO

Hespel, Maltoni, Vryonidou 15; Les Houches 19

caused by new kinematic region in real radiation:



difference of eikonal factors:

soft Z emission: $\frac{p^\mu}{p \cdot p_Z}$

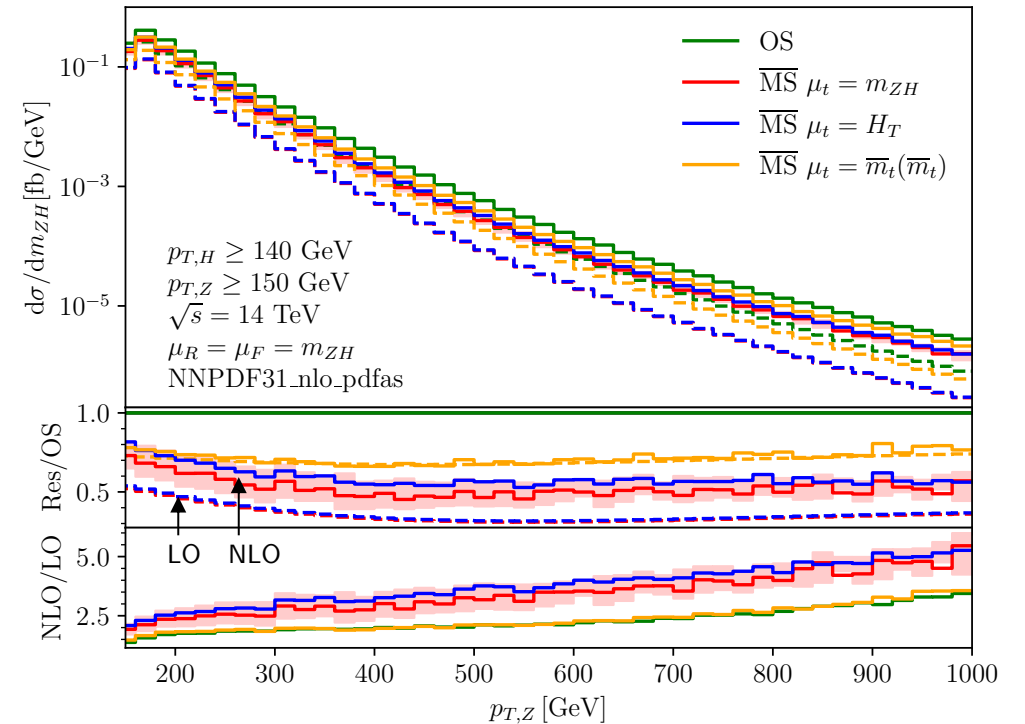
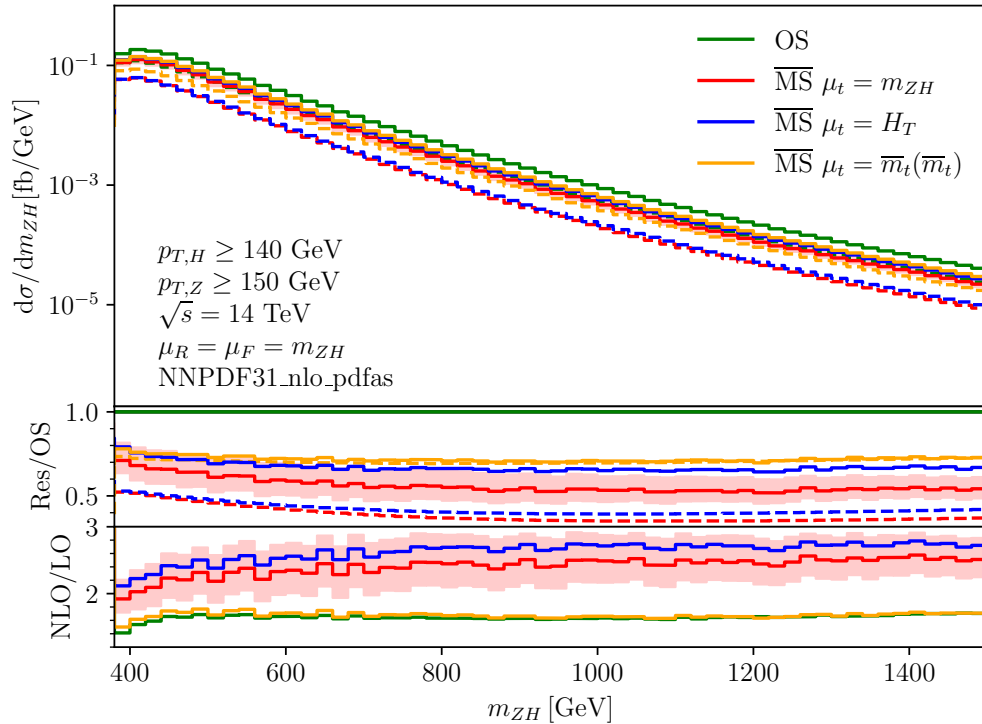
soft H emission: $\frac{m_t}{p \cdot p_H}$

→ larger enhancement of Z emission for large p_T

Mass Scheme Dependence

The results presented so far use OS renormalization of m_t , we can change to $\overline{\text{MS}}$ renormalization (using the high-energy expansion where m_t is not fixed in reduction)

$$m_t \rightarrow \overline{m}_t(\mu_t) \left(1 + \frac{\alpha_s(\mu_R)}{4\pi} C_F \left\{ 4 + 3 \log \left[\frac{\mu_t^2}{\overline{m}_t(\mu_t)^2} \right] \right\} \right)$$



The $\overline{\text{MS}}$ result is significantly smaller than OS result:

LO: ~ factor 2.9
 NLO: ~ factor 1.9
 at $m_{ZH} = 1$ TeV

If taken as uncertainty, it is much larger than scale dependence

Mass Scheme Dependence

Leading HE contributions in $gg \rightarrow HH$ and $gg \rightarrow ZH$ production

$$A_i^{\text{fin}} = a_s A_i^{(0),\text{fin}} + a_s^2 A_i^{(1),\text{fin}} + \mathcal{O}(a_s^3)$$

HH

$$A_i^{(0)} \sim m_t^2 f_i(s, t)$$

$$A_i^{(1)} \sim 6C_F A_i^{(0)} \log \left[\frac{m_t^2}{s} \right]$$

LO: m_t^2 from y_t^2

NLO: leading $\log(m_t^2)$ from mass c.t.
converting to \overline{MS} gives $\log(\mu_t^2/s)$

motivating scale choice of $\mu_t^2 = s$

ZH

$$A_i^{(0)} \sim m_t^2 f_i(s, t) \log^2 \left[\frac{m_t^2}{s} \right],$$

$$A_i^{(1)} \sim \frac{(C_A - C_F)}{6} A_i^{(0)} \log^2 \left[\frac{m_t^2}{s} \right]$$

LO: one m_t from y_t

NLO: leading $\log(m_t^2)$ not coming
from mass c.t.

→ The leading contributions seem to have different origins for the 2 processes

It would be interesting to understand these logarithms in more detail.
(for some recent progress for off-shell H production, see [Liu, Modi, Penin 21](#); [Mazzitelli 22](#))

Conclusion

NLO corrections to ZH production in gluon-fusion

Virtual corrections obtained from combination of 2 calculations

- numeric evaluation using pySecDec
- high-energy expansion

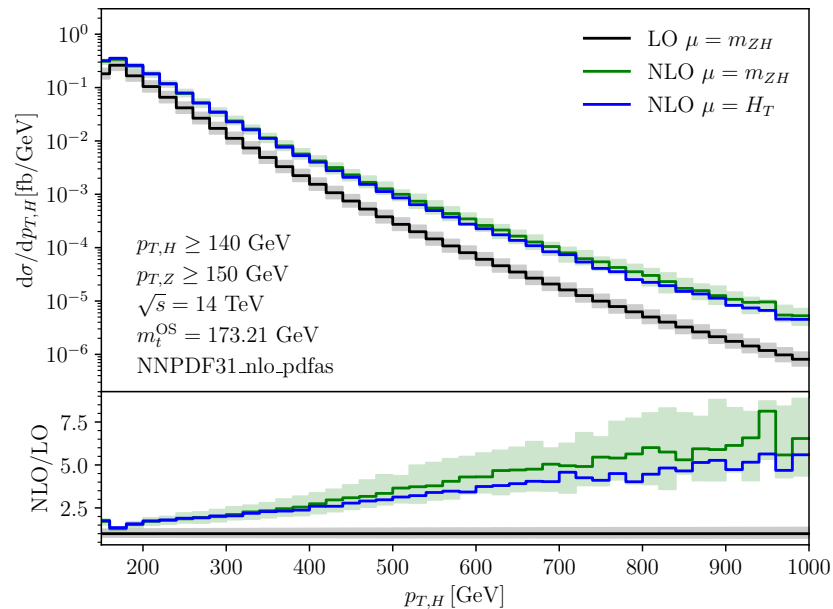
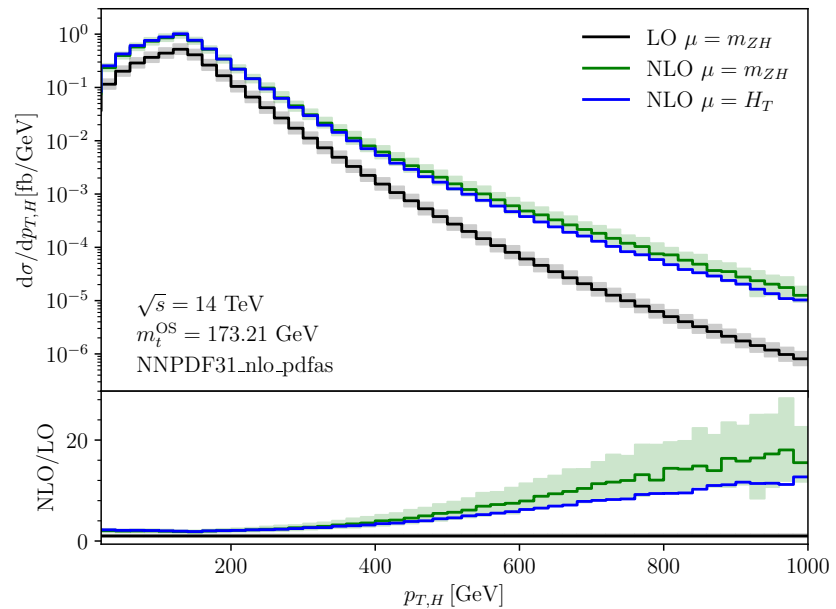
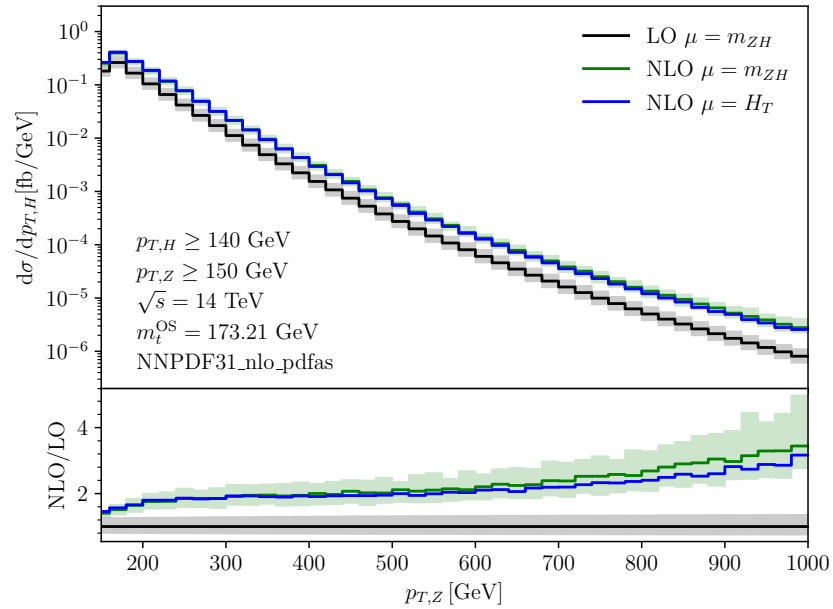
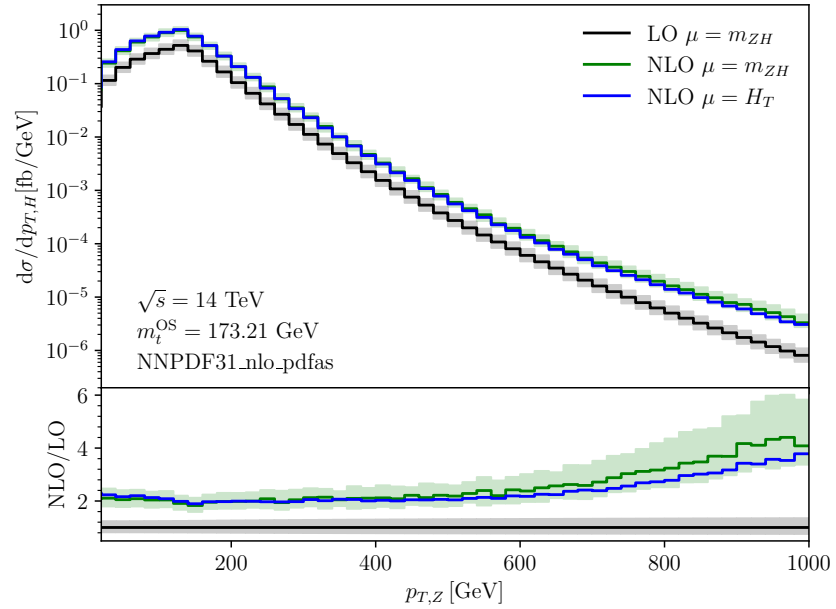
Phenomenological results

- K-factor ≈ 2
- large corrections at high- p_T due to new kin. configurations
- large dependence on top-mass renormalization scheme

Thank you for your attention!

Backup

Results – p_T distributions



Size of this effect reduced with additional p_T cuts, but K-factor still large, ~ 5